ATAD2 is a potential immunotherapy target for patients with small cell lung cancer harboring HLA-A*0201

Li Yuan,[a] Sini Li,[c] Yixiang Zhu,[a] Lin Yang,[b] Xue Zhang,[a] Yan Qu,[d] Zhijie Wang,[a] Jianchun Duan,[a] Jia Zhong,[a] Yanhua Tian,[a] Lihui Liu,[a] Boyang Sun,[a] Kailun Fei,[a] Zheng Liu,[a] Jian Zhang,[a] Yan He,[a] Yufeng Guo,[a] DanMing He,[a] Wei Zhuang,[a] Jinsong Zhang,[a] Zixiao Ma,[a] Hua Bai,[a] and Jie Wang[a,*]

[a]State Key Laboratory of Molecular Oncology, CAMS Key Laboratory of Translational Research on Lung Cancer, Department of Medical Oncology, National Cancer Centre/National Clinical Research Centre for Cancer/Cancer Hospital, Chinese Academy of Medical Sciences Peking Union Medical College, Beijing, 100021, China
[b]Department of Pathology, National Cancer Centre/National Clinical Research Centre for Cancer/Cancer Hospital, Chinese Academy of Medical Sciences and Peking Union Medical College, Beijing, 100021, China
[c]Department of Medical Thoracic Oncology, Zhejiang Cancer Hospital, Hangzhou Institute of Medicine (HIM), Chinese Academy of Sciences, Hangzhou, Zhejiang, 310022, China
[d]Department of Radiotherapy, Shandong Provincial Hospital Affiliated to Shandong First Medical University, Jinan, Shandong, 250021, China

eBioMedicine
2025;112: 105515
Published Online xxx
https://doi.org/10.1016/j.ebiom.2024.105515

Summary

Background Small cell lung cancer (SCLC) represents a highly aggressive neuroendocrine tumour with a dismal prognosis. Currently, the identification of a specific tumour antigen that can facilitate immune-based therapies for SCLC remains elusive.

Methods We employed liquid chromatography–tandem mass spectrometry (LC–MS/MS) to analyse cancer/testis antigens (CTAs) in SCLC cell lines and human tumour specimens. Immunohistochemistry of clinical specimens was performed to compare protein expression in SCLC, non-small cell lung cancer (NSCLC), and matched normal-adjacent tissues. Additionally, publicly available RNA sequencing databases were interrogated to identify gene expression patterns in different SCLC subtypes and in different disease stages.

Findings Distinct numbers and types of CTAs were identified across SCLC subtypes, with significantly higher expression levels of ATPase family AAA domain-containing protein 2 (ATAD2) observed in SCLC compared to normal adjacent tissues and NSCLC tissues. A dynamic expression pattern of ATAD2 was found throughout the clinical course of SCLC and exhibited a positive correlation with achaete-scute family bHLH transcription factor 1 (ASCL1) expression in SCLC. Immunopeptidomics analysis identified the YSDDDVPSV sequence derived from the HLA-A*02:01 restriction epitope of ATAD2 as a highly promising tumour antigen candidate for potential immunotherapy applications. YSDDDVPSV immunopeptides were confirmed to be present in SCLC-A and SCLC-N with HLA-A*02:01 restriction. Notably, HLA-A*02:01 T cells exhibited a robust response upon stimulation with YSDDDVPSV immunopeptide pulsed by T2 cells.

Interpretation Our findings highlight the potential of targeting the ATAD2 YSDDDVPSV immunopeptide for SCLC immunotherapy, thereby offering a promising avenue for the development of adoptive T cell therapies to effectively treat ASCL1-positive or NEUROD1-positive SCLC carrying HLA-A*02:01.

Funding This study was supported by the National key R&D program of China (2022YFC2505000); National Natural Science Foundation of China (NSFC) general program (82272796) NSFC special program (82241229); CAMS Innovation Fund for Medical Sciences (CIFMS 2022-I2M-1-009); CAMS Key Laboratory of Translational Research on Lung Cancer (2018PT31035); Aiyou foundation (KY201701). National key R&D program of China (2022YFC2505004). NSFC general program (81972905). Medical Oncology Key Foundation of Cancer Hospital Chinese Academy of Medical Sciences (CICAMS-MOCP2022012).

*Corresponding author. State Key Laboratory of Molecular Oncology, CAMS Key Laboratory of Translational Research on Lung Cancer, Department of Medical Oncology, National Cancer Centre/National Clinical Research Centre for Cancer/Cancer Hospital, Chinese Academy of Medical Sciences Peking Union Medical College, Beijing, 100021, China.
E-mail address: zlhuxi@163.com (J. Wang).

Keywords: Small cell lung cancer (SCLC); Cancer/testis antigens (CTAs); ATPase family AAA domain-containing protein 2 (ATAD2); HLA-A*02:01; Immunopeptidomics; YSDDDVPSV

Research in context

Evidence before this study

In SCLC, the survival benefit of immune-based therapy is limited to a specific subset of patients because of high heterogeneity among the molecular and clinicopathologic characteristics of this tumour type. Despite concerted efforts, driver mutation genes other than TP53 and RB1 deletions have yet to be identified in SCLC, leading to a lack of tumour antigen targets to expand immune-based therapy options. CTAs are TAAs that have low or absent expression in most normal tissues, but are abundant in a wide range of malignant cells, making CTAs attractive antigenic targets. ATAD2, a CTA belonging to the AAA + ATPase and bromodomain family of proteins, is a newly identified oncogene that exhibits oncogenic functions in a wide range of malignancies. ATAD2 has established roles in promoting tumourigenesis and development, but its precise function in tumour immune evasion and potential utility as an immunotherapy target remain ambiguous.

Added value of this study

ATAD2 is expressed at significantly higher levels in SCLC than in matched normal-adjacent tissue or in NSCLC tissues. There is significant variation in *ATAD2* expression among SCLC subtypes, with significantly higher *ATAD2* expression in SCLC-A/N tumours. We describe YSDDDVPSV as a novel antigenic peptide of ATAD2 that may enable successful therapeutic targeting of ASCL1-positive or NEUROD1-positive SCLC carrying HLA-A*02:01.

Implications of all the available evidence

Targetable antigens expressed by SCLC have not been identified, preventing the use of immunotherapy drugs for this indication. TCR-T is a type of adoptive cell transfer (ACT) therapy that is generating great excitement in the field of tumour immunotherapy, and selection of an appropriate tumour antigen target is key to developing safe and effective TCR-T cell therapies. These findings offer the promise of a novel opportunity to explore TCR-T to treat a subset of SCLC.

Introduction

Small cell lung cancer (SCLC) is an aggressive malignancy characterized by high metastatic potential and poor prognosis.[1] Recent incorporation of immune checkpoint inhibitors (ICIs) into platinum-based chemotherapy has revolutionized the treatment paradigm for SCLC.[2] Several large randomized phase III trials, such as IMpower133, CASPIAN, ASTURM, and CAPSTONE-1, have all shown a consistent survival benefit from the addition of PD-1/PD-L1 inhibitors to the frontline regimen for SCLC.[3–7] Recently, long-term follow-up data from the aforementioned studies have been reported, revealing a 3-year survival rate of 17.8% in the combined therapy arm compared to 5–6% in the chemotherapy control arm. These data imply that only a subset of patients with ES-SCLC obtains durable benefits from immunotherapy. Therefore, refining subtypes based on heterogeneity is extremely important for guiding therapy selection in SCLC.

However, the survival benefit of immune-combined therapy is limited to a specific subset of patients because of the high heterogeneity of the molecular and clinicopathologic characteristics of SCLC.[8] In recent years, multiple research teams have been investigating and optimizing subtypes of SCLC, proposing refined subtype categorizations such as SCLC-A/N/P/I or SCLC-A/N/P/Y and mixed, based on the expression levels of key transcription factors.[9–11] Subsequent studies identified potentially distinct therapeutic vulnerabilities of the corresponding subtypes. For instance, the SCLC-I or SCLC-Y subtype was found to show greater efficacy in PD-1/PD-L1 inhibitor treatment due to high expression of multiple immune genes, markers of T cell infiltrate, and increased expression of HLA genes.[12] Meanwhile, SCLC-A/N/P subtypes might be sensitive to B-cell lymphoma 2 (BCL2) inhibitors (BCL2i), aurora kinase (AURK) inhibitors (AURKi), and PARP inhibitors (PARPi), respectively.[11] However, apart from SCLC-I, the potential efficacy of immunotherapy in other SCLC subtypes remains uncertain. Unfortunately, immunotherapy drugs have been unable to fully overcome the state of abnormal T cell function in the immune compartment of SCLC tumours. To date, there are no effective immunotherapy treatments for patients with SCLC. Adoptive cell transfer (ACT) therapy, which includes tumour-infiltrating lymphocyte (TIL) therapy, T cell receptor (TCR) T-cell therapy, and Chimeric Antigen Receptor (CAR) T-Cell therapy, has been highly successful in cancer treatment as an approach to address abnormal T-cell function in the tumour microenvironment.[13] CAR is MHC-independent and can only detect surface antigens on the plasma membrane; therefore, CAR-T cells have significantly lower antigenic sensitivity compared to TCR-T cells, which are MHC-dependent and can be activated by fewer than 50 MHC molecules.[13,14] In clinical application, CAR-T cells were found to be more prone to inducing cytokine storm than TCR T-cell therapy.[15,16] Therefore, targeting tumour antigens and constructing TCR-T cells with specific recognition and killing ability has become a highly promising

therapeutic modality,[17] but TCR-T cell therapy has not been studied in SCLC. Therefore, investigating specific tumour antigens (neoantigens) each distinct subtype of SCLC could be crucial to addressing this unresolved question. Despite concerted efforts, driver mutation genes other than TP53 and RB1 deletions have yet to be identified in SCLC, leading to a lack of tumour antigen targets for effective immunotherapy.[18]

Cancer/testis antigens (CTAs) are tumour-associated antigens (TAAs) expressed mainly in cells of testis and embryonic tissues. Although CTA expression is low or absent in other normal tissues, it is abundant in a wide range of malignant cells—where they are expressed in a variety of tumours without organ specificity—making CTAs a potential antigenic target for early detection and immunotherapy of many tumours.[19] The advent of high-throughput polymerase chain reaction (PCR) and sequencing technologies has greatly facilitated the identification CTAs by autologous genotyping.[20] The number of identified CTAs has increased rapidly, with more than 281 CTA genes indexed in public databases (http://www.clinicaltrials.gov). CTAs were identified as one of the most potent tumour antigens for inducing both the cellular and humoral immune responses in the host.[21] Several clinical trials are currently underway using MAGE or NY-ESO-1 antigenic peptides identified from CTAs to elicit cellular and/or humoral immune responses against various cancer types.[22,23]

ATAD2, a CTA belonging to the AAA + ATPase and bromodomain family of proteins, is a newly identified oncogene that exhibits oncogenic functions in a wide range of malignancies.[24] Multiple studies reported the oncogenic function of ATAD2 in a variety of signaling pathways, including p53-mediated and p38-MAPK-mediated apoptosis pathways,[25] the AKT pathway,[26] the RB/E2F-cMYC pathway,[27] the epithelial-to-mesenchymal transition (EMT) pathway,[28] and the steroid hormone signaling pathway.[29] Furthermore, ATAD2 has been implicated in chromatin dynamics, DNA replication, and gene transcription processes, exerting its role as an epigenetic reader and transcription factor or co-activator to promote tumourigenesis.[30–34]

Despite well-documented expression of CTAs/ATAD2 in a variety of malignant tumours and its established roles in promoting tumourigenesis and development, the precise function of this tumour-associated antigen and its involvement in tumour immune evasion and immunotherapy remain ambiguous. Furthermore, there is a lack of knowledge regarding the potential contribution of ATAD2 as immunotherapy targets across various subtypes of SCLC. Therefore, the primary objective of this study is to identify and characterize the types of CTAs present in SCLC, with a specific focus on elucidating the expression patterns and biological functions of ATAD2 across the five distinct SCLC subtypes. Additionally, we aim to investigate ATAD2 and its derived immune peptides as potential targets for immunotherapy in SCLC.

Methods

Patient selection

One hundred and seven patients who underwent surgery after being diagnosed with SCLC and 73 patients who underwent surgery after being diagnosed with NSCLC at CHCAMS between 2010 and 2019 were recruited, among which 80 patients had pure SCLCs (p-SCLCs), 27 patients had combined SCLCs (c-SCLCs); 54 patients had lung adenocarcinoma (LUAD); and 19 patients had lung squamous cell carcinoma (LUSC). Clinical data (including age, sex, smoking history, and stage by Veterans Administration Lung Study Group [VALSG]) were exported from the medical records system.

Cell culture and cell lines

Fifteen human SCLC cell lines obtained from the Cell Resource Centre, Peking Union Medical College, which is part of the National Science and Technology Infrastructure, National Biomedical Cell-Line Resource (NSTI-BMCR) (NCI-H69, SHP77, NCI-H82, NCI-H524, DMS53, and NCI-H1048), American Type Culture Collection (NCI-H889, NCI-H146, NCI-H446, NCI-H526, SW1271, DMS114, NCI-H196 and NCI-H2066), and the Japanese Cancer Research Resources Bank (SBC2). NCI-H2066 is a cell line exhibiting epithelial morphology that was isolated from patient with small cell lung cancer and adenocarcinoma. NCI-H69 and SHP77 were maintained in RPMI 1640 (Biological Industries [BI]) medium supplemented with 20% fetal bovine serum (BI). NCI-H889, NCI-H146, NCI-H82, NCI-H524, NCI-H446, NCI-H196, and NCI-H526 were cultured in RPMI 1640 (Gibco) supplemented with 15% Gibco serum. NCI-H2066, SW1271, DMS53, NCI-H1048, DMS114, and SBC2 were cultured in DMEM/F12 (Gibco) supplemented with 10% Gibco serum, insulin-transferrin selenium (Gibco), 10 nM hydrocortisone (Sigma-Aldrich), and 10 nM β-estradiol (Sigma-Aldrich). All cells were cultured at 37 °C in a 5% CO_2 humidified incubator.

Preparation of peptides from DMS53 SCLC cells

DMS53 cells, which do not express HLA-I, were centrifuged and resuspended in 50-ml test tubes, and then all cell suspensions were combined in a single tube filled with culture medium up to 50 ml. The appropriate amount of water containing 10 μl/ml protease-inhibiting PMSF was added to the cell pellet and aliquot the cell suspension equally into cryostat tubes (approximately 1 ml per tube). The cryostat was immersed into a liquid nitrogen tank for at least 3 min before it was thawed in a 37 °C water bath, and this freeze-thaw process was repeated twice to completely lyse cells. After centrifugation at 410*g* for 5 min at 4 °C, the supernatant was carefully removed with a pipette and filtered through a 0.22-μm syringe filter and set aside.

Maturation of dendritic cells from peripheral blood mononuclear cells

Normal volunteer peripheral blood mononuclear cells (PBMCs) were separated and cultured using AIM-V (Gibco, 087-0112DK) medium for 4 h, and the cells were observed with a microscope to see if they were attached to the bottom of the culture flasks, followed by gentle shaking of the culture flask 10 times to suspend the non-adherent cells. The suspended cells were transferred to a 50-ml tube and AIM-V supplemented with 1×10^6 U/ml GM-CSF and 1.0×10^6 U/ml IL-4 was added to the adherent cells remaining in the flask for 3 days' additional culturing. On the third day of culturing, 1 ml of cancer cell lysate was added to each culture flask to stimulate dendritic cell (DC) maturation.

Sample preparation and liquid chromatography–tandem mass spectrometry analysis

Cell lysis buffer was added to ten cultured SCLC cell lines (NCI-H69, SHP77, NCI-H889, NCI-H146, NCI-H82, NCI-H446, NCI-H526, DMS114, NCI-H196 and NCI-H2066) and to DCs presenting DMS53 antigens. The mixture was incubated on ice for 60 min, followed by a 5-min sonication and high-speed centrifugation at 20,000*g* for 1 h at 4 °C to collect the supernatant. The supernatant was then subjected to enrichment and elution of HLA-peptide complexes (HLA-I) using an NEO Discovery HLA-I Peptide Enrichment Kit (Baizhen Biotechnologies). The HLA-peptide complexes were then separated using a reverse-phase column to obtain immunopeptide fractions. The collected fractions were analysed by LC–MS/MS.

Mass spectrometry data acquisition was performed using a Nano-Elute high-performance liquid chromatography system. The immunopeptidome was analysed with a high-resolution mass spectrometer (Bruker timsTOF Pro2). The instrument parameters used were as follows: acquisition mode: DDA; total run time: 60 min; full mass scan range: m/z 100–4000; the setting of PASEF: 10 MS/MS (total cycle time 2.22 s); and ion intensity threshold: 2500. Then, the raw mass spectrometry files (.d) were generated. All raw data files collected by mass spectrometry were analysed with the PEAKS DeepNovo Peptidome (Bioinformatics Solutions, Inc.) against a database of the human sequences in UniProt and SwissProt, in which de novo sequencing, database search, and homology search are combined for peptide identification. On this platform, the SPIDER algorithm is specially designed to detect peptide mutations, through which sequence variants and mutations that were defined as homologs could be identified. Those peptides that could not be found in the protein database were defined as DeepNovo, and the average local confidence (ALC%) score of each peptide was chosen to be >50%. No enzyme digestion was selected because HLA peptides are natural peptides without artificial enzyme digestion. Precursor mass and fragment ion mass tolerances were set as 20.0 ppm and 0.05 Da, respectively. Methionine oxidation (15.99 Da) was set as variable modifications, and false discovery rate (FDR) was set as 1%. Peptides with a length between 7 amino acids and 16 amino acids were selected. A DeepImmu Neoantigen Discovery platform (Bioinformatics Solutions, Inc.) was used for immunogenicity prediction of immunopeptides. Eluted ligand rank (EL_rank): strong binders were defined as having EL_rank ≤0.5 and weak binders as having 0.5 <EL_rank ≤2.

IHC staining

Lung tissue slides with 4–5-mm tissue sections from 80 patients with p-SCLC, 27 patients with c-SCLC and 73 patients with NSCLC were baked at 60 °C, deparaffinized with xylene, and rehydrated through a graded series of ethanol solutions (100%, 95%, 85%, and 75%). Tissue slides were then treated with microwaves to induce epitope retrieval by boiling slides in citric acid solution or Tris/EDTA buffer for 20 min. Protein blocking was performed using blocking buffer (ZSGB-BIO, GT101510) for 30 min at room temperature. Primary antibodies for anti-Mash1/achaete-scute homolog (Abcam, ab211327), anti-NeuroD1 (Abcam, ab213725), anti-Pou2f3 (Novus Biologicals, NBP1-83966), anti-YAP1 (Abcam, ab205270), and anti-ATAD2 (Cell Signaling Technology, 50563) were used. The slides were incubated with secondary antibodies (HRP-anti-rabbit IgG, ZSGB-BIO, PV-6001; HRP-anti-mouse IgG, ZSGB-BIO, PV-6002) for 30 min at 37 °C. Each slide was evaluated by three pathologists.

IHC scoring

Expression of ASCL1, NEUROD1, POU2F3, YAP1, and ATAD2 were quantified by H-score, which was calculated by the multiplication of the different staining intensities in four gradations (range, 0–3) with each percentage of positive cells. We translated the continuous H-score into the four gradations: H-score 0–9 (–); H-score 10–49 (1+); H-score 50–149 (2+); and H-score 150–300 (3+). Therefore, the expression of ASCL1, NEUROD1, POU2F3, YAP1, and ATAD2 was defined as negative (–) when the H-score was <10 and positive (1+/2+/3+) when the H-score was ≥10.

Western blotting

Cells were lysed in RIPA buffer (Beyotime, P0013B). Protein concentration was measured using a Bicinchoninic Acid (BCA) Protein Assay Kit (Thermo-Fisher Scientific, 23227), and the lysates were subjected to SDS–PAGE gel electrophoresis and transferred onto PVDF membranes. Membranes were probed using the following primary antibodies: anti-Mash1/achaete-scute homolog (Abcam, ab211327), anti-NeuroD1 (Abcam, ab213725), anti-Pou2f3 (Novus Biologicals, NBP1-83966), anti-YAP1 (Abcam, ab205270), anti-ATAD2

(Cell Signaling Technology, 50563), anti-HLA class I ABC (Abcam, ab70328), anti-HLA-DR + DP + DQ (Abcam, ab7856), anti-beta-2 microglobulin (ABclonal, A1562), anti-TAP1 (ABclonal, A6213), anti-TAP2 (ABclonal, A1610), anti-ERAP1 (ABclonal, A5978), anti-CIITA (Cell Signaling Technology, 3793), and anti-β-actin. Primary antibodies were diluted in 5% non-fatty milk or primary antibody dilution (Beyotime, P0256) in TBST at 1:1000 and incubated overnight at 4 °C, followed by HRP-conjugated secondary antibody incubation at room temperature for 2 h. Secondary antibodies used included: goat anti-rabbit HRP-conjugated IgG (Abcam, ab6721) and rabbit anti-mouse HRP-conjugated IgG (Abcam, ab6728). Images were collected by an Amersham Imager 600 (General Electric).

Flow cytometry

To quantify antigens, fresh tumour cell lysates were stained with conjugated antibodies and isotype controls. The antibodies used included: FITC human HLA-ABC antibody (Invitrogen, 11-9983-42), PE human HLA-ABC antibody (Invitrogen, 12-9983-42), FITC mouse IgG2a kappa isotype control (Invitrogen, 11-4724-42), FITC human CD14 antibody (BioLegend, 325604), FITC human CD40 antibody (BioLegend, 334306), FITC human CD86 antibody (BioLegend, 374204), FITC mouse IgG1 kappa iotype control (BioLegend, 400108), PE human CD11c antibody (BioLegend, 337206), PE human CD83 antibody (BioLegend, 305308), PE human CD80 antibody (BioLegend, 375410), PE mouse IgG1 kappa isotype control (BioLegend, 400112), Per-CP/Cyanine5.5 human HLA-DR antibody (BioLegend, 327020), and PerCP/Cyanine5.5 human CD3 antibody (BioLegend, 317336). After staining, immunocyte analysis was performed on an LSR II (BD Biosciences).

HLA high-resolution genotyping

A TBG HLAssure SE A Locus SBT Kit (cat. no. 50110) was used to analyse high-resolution HLA-A typing results by collecting SCLC cell lines for DNA extraction. The A260/A280 ratio for nucleic acid samples was between 1.65 and 1.8. After PCR, a colloid electrophoresis reaction was performed, followed by PCR product purification (ExoSAP-ITTM), PCR product quality determination based on molecular weight of PCR amplification products on an electropherogram, and sequencing of the precipitated DNA fragments. The alleles were analysed using an AccuType (BioSoft). The results were interpreted as follows: (1) HLA alleles with the same nucleotide sequence in exons coding for the peptide binding domain (exon 2 and exon 3 for HLA class I and exon 2 for HLA class II) were assigned to Group G and named by adding a capital G to the first three digits of the lowest numbered allele; (2) HLA alleles in which the peptide binding domain (exon 2 and exon 3 for HLA class I and exon 2 for HLA class II) encodes the same nucleotide sequence and results in the same protein sequence were assigned to Group P and named using the first two digits of the lowest numbered allele plus an uppercase P.

PBMC isolation from healthy donors and HLA typing

PBMCs from two healthy volunteers were isolated from whole blood samples. In brief, 15 ml of lymphocyte isolation solution was added into the lower chamber of a 50-ml separator tube, and 20 ml of diluted blood sample was then added. Samples were centrifuged at 1200*g* for 15 min at 4 °C. After centrifugation, the sample in the tube was layered from top to bottom as follows: plasma—white membrane layer—separator—septum—separator—erythrocyte precipitate. The liquid in the upper layer of the septum was poured into another sterile centrifuge tube and PBS was added to 45 ml. Next, the washed cells were resuspended with a pipette, and centrifuged at 300*g* for 10 min at room temperature. The wash was repeated once or twice, and the obtained single nucleated cells were frozen or subjected to downstream analysis and culture, including HLA typing. One sample was positive for HLA-A*02.01 and one sample was negative (non-HLA-A*02:01).

Stimulation of PBMCs with T2 cells pulsed with YSDDDVPSV peptide

T2 cell is a transporter associated with antigen processing (TAP)-deficient human HLA-A2+ cell line that can be efficiently loaded with exogenous peptides. PBMCs were resuspended in T cell medium (RPMI 1640 supplemented with 10% FBS, 2 mmol/L L-glutamine, and 50 μmol/L 2- mercaptoethanol) at a density of 5×10^6 cells per 1 ml of medium in a six-well plate. IL-2 was added to the medium on day 0 at 20 U/ml. Cultures were stimulated using irradiated (70 Gy) T2 cells loaded with 100 μmol/L of the YSDDDVPSV peptide for 48 h. Enrichment of T cell activation-related markers was performed before the cultured PBMCs were restimulated. Restimulation involved plating the cells at a density of 2×10^6 per 1 ml in a 24-well plate containing IL-2 at a concentration of 20 U/ml. Irradiated (70 Gy) T2 cells loaded with 100 μmol/L YSDDDVPSV peptide were used again to stimulate the cultured PBMCs. Autologous PBMCs irradiated by 30-Gy rays were used as a feeder layer and cultured for an additional 7 days before the cells were collected for interferon γ (IFN-γ) analysis as detailed below.

Cytokine detection

Cytotoxic T lymphocyte (CTL) cells (2×10^5) were stimulated with 2×10^5 YSDDDVPSV peptide-coated T2 cells (1:1 ratio) in triplicate in a 96-well plate. After incubation for 24 h, the supernatant was collected according to the manufacturer's instructions, and IL-5, IFN- α, IL-2, IL-6, IL-18, IL-10, IFN- γ, IL-8, IL-17, IL-4, IL-12P70, and TNF-α cytokines were detected using a

human CBA detection kit, a human cytokine panel, and cytometric bead array (CBA) (IL-5, IFN-α, IL-2, IL-6, IL-18, IL-10, IFN-γ, IL-8, IL-17, IL-4, IL-12P70, and TNF-α) (BioLegend, LEGENDplex Human Multi-Analyte Flow Assay Kit). At the same time, the incubated cells were collected and stained with human CD8 antibody. After breaking the cell membrane with FIX&PERM antibody cell permeabilization reagents (Invitrogen, GAS003), the cells were stained with human IFN-γ antibody. Intracellular cytokine staining (ICS) and CBA were performed according to the manufacturer's instructions. The antibodies and related reagents used included: PE human HLA-A2 antibody (BioLegend, 343305), APC human CD8 antibody (BioLegend, 300912); and FITC human IFN-γ antibody (BioLegend, 502505). Anti-PE MicroBeads (Miltenyi Biotec, 130-048-801) and LS separation columns (Miltenyi Biotec, 130-042-401).

Bioinformatic analysis

The single-cell RNA sequencing (scRNA-seq) data from human SCLC lung tissues[31] were retrieved from the Genome Sequence Archive database of the National Genomics Data Centre (https://bigd.big.ac.cn/). The Seurat object of single-cell transcriptomic atlas was plotted by the R package ggplot2 (version 3.5.0), and plotDensity was used to visualize the distribution of markers. In addition, the subset of cell type and tumour was selected to calculate the bulk expression using the AggregateExpression function. The between-gene correlations were calculated and then displayed using pheatmap.

GSM4104155 (untreated CTC), GSM4104156 (cisplatin CTC), GSM4104157 (cisplatin relapsed CTC), and GSM4104163 (untreated CDX) single-cell data were downloaded from the Gene Expression Omnibus (GEO) database under accession number GSE138267. First, all 10× Genomic data were merged; cell quality control (QC) was taken as nFeature >200 and nFeature <5000; mitochondrial ratio MT <15 as a threshold to filter low-quality cells for downstream analyses; and single-cell analyses of CTCs collected from patients at different time points were carried out using Seurat (version 5). Considering the heterogeneity of tumour cells, the top 2000 highly variable genes (HVGs) were directly selected for PCA dimensionality reduction analysis; the top 30 principal components were selected for Uniform Manifold Approximation and Projection (UMAP visualization; the FindNeighbours community method was used to search for neighbours; FindClusters was used for cell clustering; and resolution was set to 0.4. Feature plots and violin plots were generated using ggplot2 (3.5.0) and ggpubr (0.6.0).

The National Cancer Institute (NCI) SCLC cell line expression data were downloaded from the GEO (GSE73160). The normalized expression data were used for visualizing the marked change of ATAD2 across cell lines from low expression level to high expression level using ggplot2 (version 3.5.0). Gene expression data with accession numbers GSE43346 and GSE40275 were downloaded from the GEO using GEOquery, normalized by $\log_2$+1 on the expression matrix, annotated using the corresponding platform GPL annotation files, and filtered for low-expression genes and then analysed for differences among NSCLC, SCLC, and Normal using limma. mRNA-seq data of SCLC patients were downloaded from cBioPortal database (U Cologne, Nature 2015, 120 total samples). The thresholds for differential genes were $P_{adj} \leq 0$ 05; logFC = 0.58. Volcano plots and heatmaps were plotted using ggplot, pheatmap, and ggpurb for differential CTA gene expression.

Statistics

Statistical tests were conducted using Pearson chi-square test if all cell size >5 and total sample size ≥40; otherwise, Fisher's test was used. If the P value is less than 0.05, it indicates that there is a significant difference between the distribution of variables and/or a significant correlation, implying that there may be non-trivial dependence or correlation between these two categorical variables. Statistical analyses were performed using R (version 4.4.1) and GraphPad Prism (GraphPad Software, Inc. version 10.2.1)). Data are presented as mean ± s.d. Statistical significance was determined as indicated in the figure legends. P values less than 0.05 were considered significant; $^{*}P < 0.05$, $^{**}P < 0.01$, and $^{***}P < 0.001$.

Ethics

This study was approved by the Ethics Committee and Institutional Review Board of Cancer Hospital, Chinese Academy of Medical Sciences (CHCAMS) (19/215-1999). Included studies had been approved by corresponding ethical review committees and all participants signed the consent forms.

Role of funders

The funders played no role in the study design, data collection, data analyses, interpretation, or writing of this manuscript.

Results

Characterization of human p-SCLC specimens and SCLC cell lines

Surgical pathology tissue specimens were collected from 80 patients with p-SCLC recruited from CHCAMS during 2010–2019 for five subtypes (SCLC-A/N/Y/P and -mixed) by immunohistochemistry (IHC) analysis to detect ASCL1, NEUROD1, POU2F3, and YAP1 expression. Clinical data (including age, sex, smoking history, and stage by VALSG) of the patients were extracted from medical records systems (Supplementary Table S1). Number of specimens according to five subtypes (SCLC-A/N/Y/P and -mixed) are shown in Fig. 1A. In total, 50 of 80 (62.5%) patients expressed ASCL1 (Fig. 1A and B).

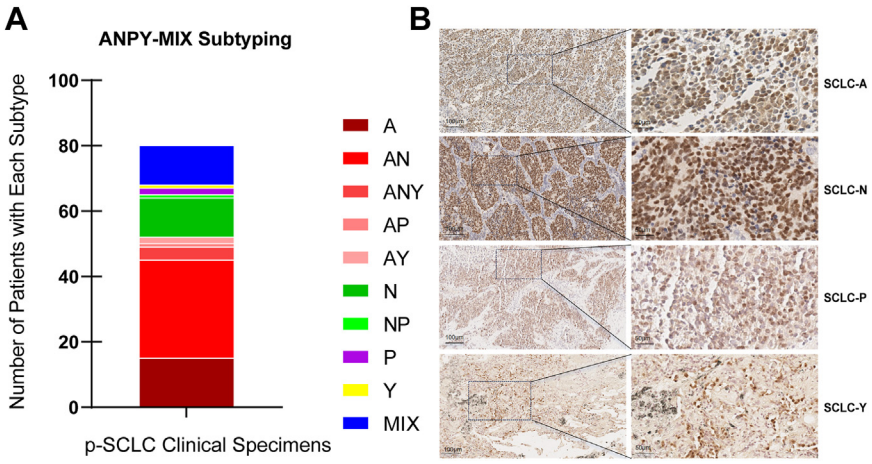

***Fig. 1:* Characterization of specimens from 80 patients with p-SCLC and 14 SCLC cell lines**. (A, B) Surgical pathology tissue specimens from patients with p-SCLC were analyzed by IHC was to detect ASCL1, NEUROD1, POU2F3, and YAP1 expression. Representative stained specimens are shown (B). Number of specimens according to five subtypes (SCLC-A/N/Y/P and -mixed); Fifteen of 80 (18.75%) specimens were identified as SCLC-A; 30 (37.5%) as SCLC-AN; four (5%) as SCLC-ANY; one (1.25%) as SCLC-AP; two (2.5%) as SCLC-AY; 12 (15%) as SCLC-N; one (1.25%) as SCLC-NP; two (2.5%) as SCLC-P; one (1.25%) as SCLC-Y; and 12 (15%) as SCLC-MIX; 50 of 80 (62.5%) specimens expressed ASCL1.

Then, we performed five subtypes (SCLC-A/N/Y/P and -mixed) of 14 SCLC cell line models by western blotting (WB), which showed four cell lines (H69, SHP77, H889, and H146) were SCLC-A, three cell lines (H82, H446, and H524) were SCLC-N subtype, one cell line (H526) was SCLC-P, and six cell lines (SW1271, DMS114, H196, DMS53, H1048, and SBC2) were SCLC-Y (Supplementary Fig. S1A and B). Next, cell surface expression of HLA-I, HLA-II, and antigen presentation machinery (APM) on the cell line models was determined by WB and flow cytometry (FCM), which showed that DMS53 and H1048 were the only cell lines that did not express HLA-I (Supplementary Fig. S1C and D). Moreover, we found that expression of HLA-I and its associated APM was lower in SCLC-A and SCLC-N subtype cell lines than in SCLC-P and SCLC-Y subtype cell lines (Supplementary Fig. S1A and B). All of the cell lines had similar expression levels of HLA-II and its associated APM (Supplementary Fig. S1A).

ATAD2 is highly expressed in SCLC patient tissues and cell lines

To identify the immune peptides in SCLC tumour cells that can be processed and presented by HLA-I, we performed LC–MS/MS analysis on 11 SCLC cell lines, representing the heterogeneity of SCLC subtypes. Ten of the cell lines were confirmed positive for HLA-I, (Fig. 2A, Supplementary Fig. S2), and one was HLA-I-deficient (DMS53). To analyse cell surface antigens on the HLA-I-deficient cells, PBMCs isolated from healthy blood donors were treated with DMS53 cell lysate and matured into DCs to present the tumour cell antigens (Supplementary Fig. S3A–D). Then, peptides from all 11 cell lines were processed and subjected to LC–MS/MS analysis. The UniProt and SwissProt human sequence databases were used to map the immunopeptides obtained from the LC–MS/MS analysis to known CTAs. A total of 99 CTAs were detected in the 11 SCLC cell lines. Among the HLA-I-expressing SCLC cell lines, SCLC-A and SCLC-N subtype cells had significantly smaller numbers of CTAs compared to SCLC-P and SCLC-Y subtype cells (Fig. 2B). The number of CTA in c-SCLC (H2066) was higher than that of p-SCLC-A/N but lower than that of p-SCLC-P/Y (Fig. 2B, Supplementary Table S2). Overall, six CTAs were common among all 11 cell lines: ATAD2, NOL4, POTEE, SPAG1, SPAG8 and TEX15 (Fig. 2B). Next, we queried scRNA-seq data from matched primary tumour, normal adjacent, and relapse tumour specimens from 11 patients with SCLC (scRNA-seq SCLC) from a previous study by our research group (Fig. 2C). We identified 85 CTAs in the primary tumour specimens (Supplementary Fig. S4A), which was similar to the number of CTAs previous reported in NSCLC tissues (96 CTAs).[35] Fewer CTAs (36) were detected in relapse tumours (Supplementary Fig. S4B), all of which were also detected in the primary tumours and in normal adjacent tissues (29) (Supplementary Fig. S4C). When compared with CTAs detected in the cell line models, we identified four CTAs (ATAD2, SPAG1, SPAG8, and NOL4) were also present in the clinical SCLC tumour specimens (Fig. 2D).

We prioritized the four common CTAs for further analysis to validate their clinical relevance. First, further analysis of the scRNA-seq SCLC 11-patient dataset showed that *ATAD2* had the highest expression, whereas *NOL4*, *SPAG1*, and *SPAG8* expression levels were lower (Fig. 3A–E). To validate this trend, we analyzed mRNA sequencing data collected from 63

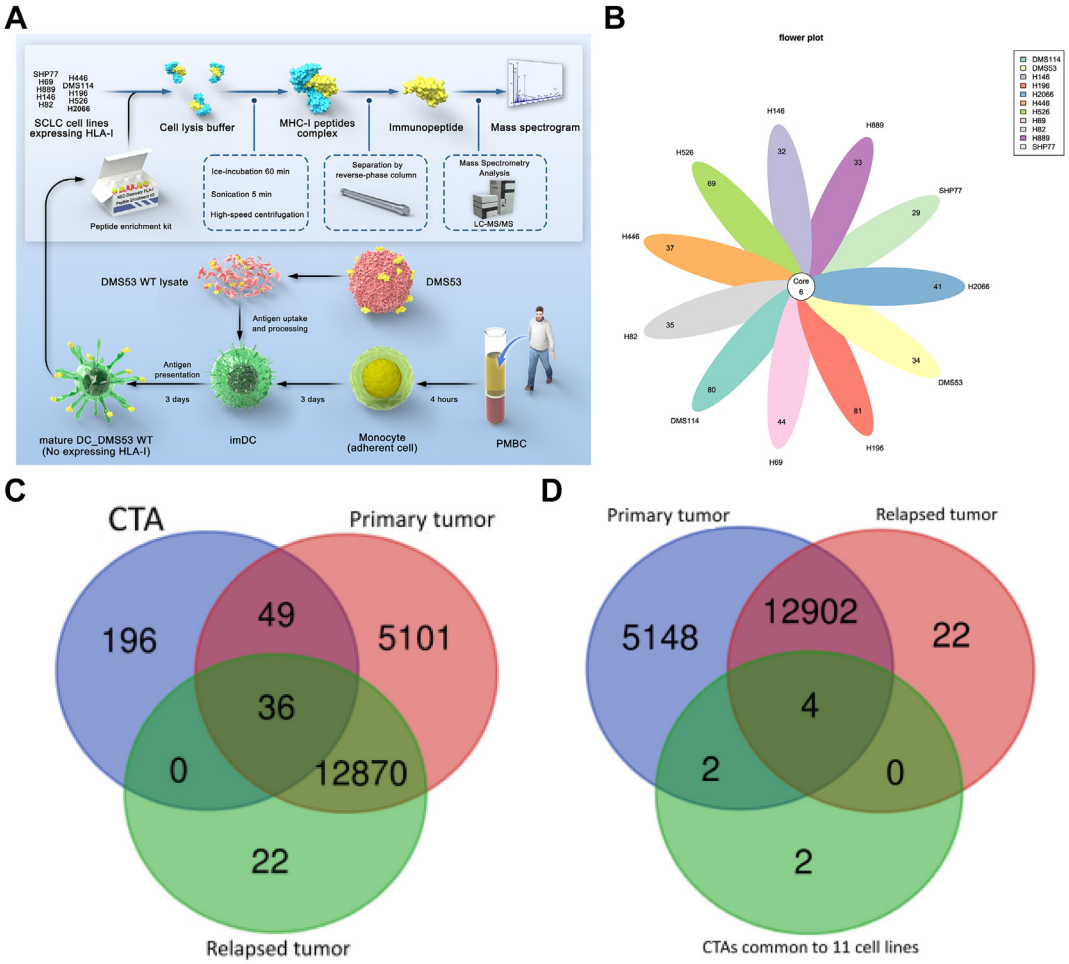

***Fig. 2:* Identification of common CTAs in different SCLC subtypes**. (A) Workflow for LC–MS/MS of immunopeptides from SCLC cell lines expressing or not expressing HLA-I. PBMCs from normal volunteers were treated with lysate from the HLA-I-deficient SCLC cell line DMS53, and peptides expressed by the mature DCs were processed by LC–MS/MS. (B) Venn diagram displaying CTAs detected in each SCLC cell line. Six CTAs were common across all 11 cell lines: ATAD2, NOL4, POTEE, SPAG1, SPAG8, and TEX15. (C) Venn diagram displaying CTAs common to 11 matched primary and relapsed tumour specimens from patients with SCLC, determined by scRNA-seq among all known CTAs (blue circle). (D) Venn diagram displaying common CTAs among 11 SCLC cell lines determined by immunopeptidomics and 11 matched primary and relapsed tumour specimens from patients with SCLC determined by scRNA-seq. Four CTAs were common across all analyses: ATAD2, SPAG1, SPAG8, and NOL4.

SCLC cell lines (GSE73160) and from SCLC patient microarray datasets (GSE43346 and GSE40275). This confirmed that the expression of *ATAD2* in both SCLC cell lines and patient tissues was markedly higher than that in the adjacent normal tissues, normal human organ tissue, and it was also higher compared to NSCLC patient tissues and cell lines (Fig. 3F–H, Supplementary Fig. S4D–G). At the protein level, IHC showed that ATAD2 expression was statistically significantly higher in 80 p-SCLC patient specimens (65.0%) than 27 c-SCLC patient specimens (25.93%) ($P < 0.001$***) and 73 NSCLC patient tissues (38.36%) ($P < 0.01$**) (Table 1). H-scores were lower in c-SCLC and NSCLC compared to p-SCLC (Fig. 3I, Table 1).

ATAD2 expression is positively correlated with the expression of ASCL1

To clarify the correlation between ATAD2 expression and five subtypes (SCLC-A/N/Y/P and -mixed) as well as with clinical characteristics of SCLC, we first evaluated scRNA-seq data and mRNA-seq data (cBioPortal database) from patients with SCLC. Correlation analysis of the mRNA-seq data identified significant positive correlations between ATAD2 and ASCL1 expression and between ATAD2 and NEUROD1 expression, with the former being the stronger correlation (Supplementary Fig. S4H). In the scRNA-seq dataset, *ATAD2* expression was positively correlated with the expression of *ASCL1* and *NEUROD1*, with the former being the

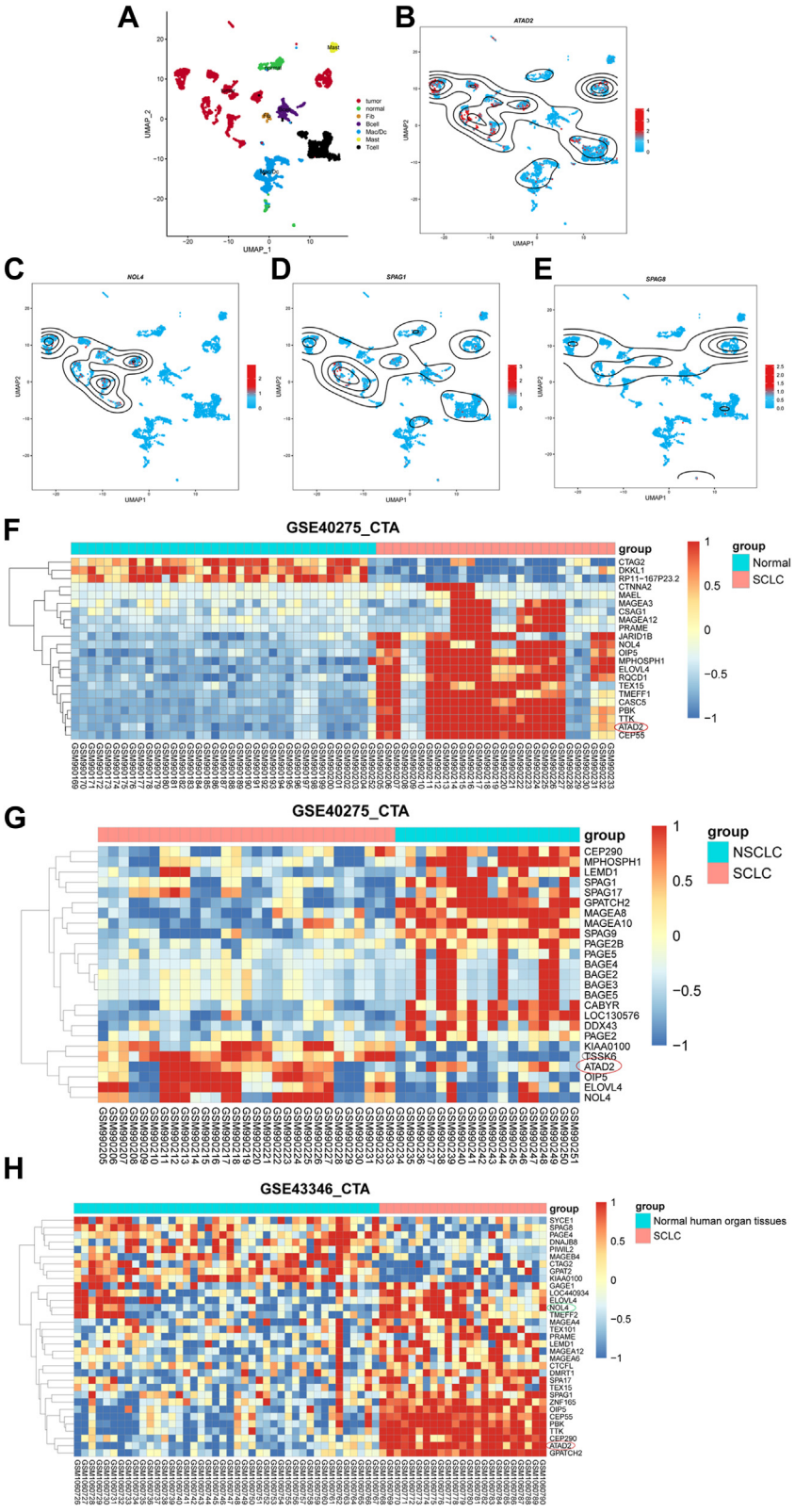

***Fig. 3: ATAD2* is highly expressed in SCLC patient tissues and cell lines and positively correlated with the expression of *ASCL1*.** (A) UMAP plot showing tumour cell clusters based on the scRNA-seq data from patients with SCLC colored by cell subtype. (B–E) *ATAD2* (B), *NOL4* (C),

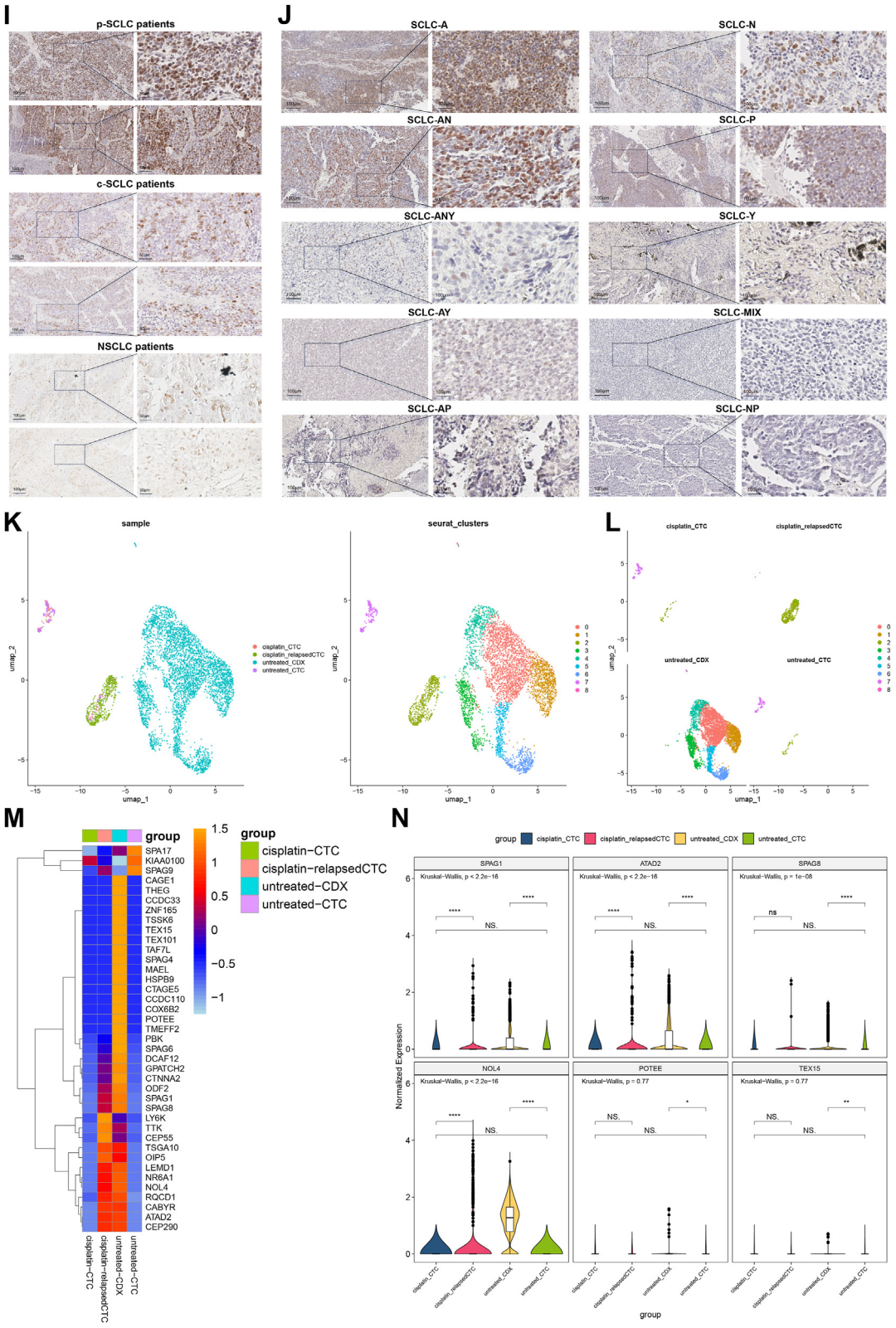

Fig. 3: Continued.

stronger correlation (Supplementary Fig. S4I). Next, we evaluated protein expression by IHC of tumour tissues from 80 patients with p-SCLC, which showed that ATAD2 expression levels varied across five subtypes (SCLC-A/N/Y/P and -mixed). Specifically, a higher percentage of SCLC-A (82.69%) and SCLC-N (65.38%) samples were ATAD2 positive compared to the other SCLC subtypes (5.76% of SCLC-P, 9.61% of SCLC-Y, and 7.69% of SCLC-MIX) (Fig. 3J). Moreover, high expression of ATAD2 was correlated with SCLC-A ($P < 0.0001$****) and negatively correlated with SCLC-MIX ($P < 0.05$*), whereas there was no correlation between ATAD2 expression level and SCLC-N, SCLC-P, or SCLC-Y (Table 2, Fig. 3J). We also did not find any correlation between ATAD2 expression and any of the clinical characteristics (age, sex, smoking history, and stage by VALSG) (Supplementary Table S1).

Finally, to study *ATAD2* expression during disease progression, we analyzed scRNA-seq data (GSE138267) collected from cell line-derived xenograft (CDX) tumours and from longitudinally collected circulating tumour cells (CTCs) from patients with SCLC before and after treatment with cisplatin. Serial scRNA-seq analyses of CTCs showed similar transcriptional heterogeneity to paired CDXs (Fig. 3K, L). *ATAD2* and *NOL4* expression was highest expression in untreated CDX and CTCs obtained from a patient after developing cisplatin resistance, while expression of these genes was low in untreated CTCs and in CTCs from patients with tumours that responded to cisplatin (Fig. 3M). *ATAD2*, *NOL4*, and *SPAG1* expression levels were higher in untreated CDX tumours than that in untreated CTCs, but lower in cisplatin-treated CTCs from responder patients compared to cisplatin-treated CTCs from patients with cisplatin resistance (Fig. 3N). These data indicate that *ATAD2* expression is dynamic, changing over the clinical course of SCLC.

Identification of YSDDDVPSV as a viable ATAD2 immunopeptide in SCLC

We analyzed immunopeptides associated with each of the ten HLA-I-expressing SCLC cell lines by LC–MS/MS (Supplementary Table S2). SCLC-A and SCLC-N SCLC cell line models had a significantly lower number of immunopeptides than SCLC-P and SCLC-Y models. The number of immunopeptides in c-SCLC (H2066) was also significantly lower than that of SCLC-P/Y (Fig. 4A). Immunopeptides were further analyzed based on HLA allele information, and we found varying numbers of immunopeptides binding to HLA-A*02:01 in H69 (522 peptides), SHP77 (49 peptides), H889 (238 peptides), and H82 (164 peptides) (Supplementary Fig. S5A). Next, we performed high-resolution HLA genotyping on ten SCLC cell lines expressing HLA-I as well as on DCs presenting antigenic peptides of DMS53 cells, which showed that H69, SHP77, H889, and H82 harbored the HLA-A*02:01 allele (Supplementary Table S3). LC–MS/MS analysis of these 10 cell lines identified 106 ATAD2 immunopeptides ranging from 7 to 16 amino acids in length, of which 104 were expressed in only one SCLC cell line. The remaining two ATAD2 immunopeptides were expressed in three SCLC cell lines: YSDDDVPSV was expressed in H69, H82, and DMS114 cells and AVTSPGQAL was expressed in H196, H526, and DMS114 cells (Fig. 4A). From these two more widely expressed immunopeptides, we considered which may make a better candidate for immune targeting. Although AVTSPGQAL (Supplementary Fig. S5C) was detected in three SCLC cell lines (H196, H526, and DMS114), it was not expressed in SCLC-A/N subtype models, and the HLA-I

SPAG1 (D), and *SPAG8* (E) expression level in SCLC patient specimens determined by scRNA-seq. (F–H) Microarray datasets were downloaded to measure CTA mRNA expression. Heatmap displaying mRNA expression of CTAs in patient SCLC and matched normal adjacent tissues (GSE40275) (F) and in SCLC and NSCLC tissues (GSE40275) (G) and in SCLC and normal human organ tissue (GSE43346) (H). *ATAD2* and *NOL4* expression are both higher in SCLC compared to adjacent normal tissues and in SCLC compared to NSCLC tissues. (I) *ATAD2* expression level in 80 human p-SCLC, 27 human c-SCLC and 73 human NSCLC specimens in the CHCAMs cohort detected by IHC. H-scores were lower in c-SCLC and NSCLC compared to p-SCLC. The expression of ATAD2 was defined as negative (–) when the H-score was <10 and positive (1+/2+/3+) when the H-score was ≥10. 52 cases with in the p-SCLC group had H-score between 10 and 240, 7 cases in the c-SCLC group had H-score between 10 and 75. 28 cases in the NSCLC group had H-score between 10 and 80. (J) ATAD2 expression level in 80 human p-SCLC specimens detected by IHC with indicated five subtypes (SCLC-A/N/Y/P and -mixed). We translated the continuous H-score into the four gradations: H-score 0–9 (–); H-score 10–49 (1+); H-score 50–149 (2+); and H-score 150–300 (3+). Therefore, the expression of ATAD2 was defined as negative (–) when the H-score was <10 and positive (1+/2+/3+) when the H-score was ≥10. Twelve cases in the SCLC-A group had H-scores between 16 and 55; four cases in the SCLC-N group had H-scores between 10 and 95; 26 cases in the SCLC-AN group had H-scores between 10 and 240; three cases in the SCLC-ANY group had H-scores between 10 and 40; two cases in the SCLC-P group had H-scores between 18 and 70; one case in the SCLC-AY group had H-scores of 75; one case in the SCLC-AP group had H-score values of 21; and four cases in the SCLC-MIX group had H-scores between 11 and 50. (K and L) UMAP display of CDX and CTC single-cell mRNA expression profiles, classified into nine clusters (right panel), which are heterogeneous among the different groups (left panel). (M) Heatmap displaying differential expression of CTAs in indicated gruops. (N) Violin plot displaying differential expression of six CTAs common across all the 11 SCLC cell lines in indicated groups. Cisplatin_CTC, $n = 124$ cells; cisplatin_relapsed CTC, $n = 511$ cells; untreated_CDX, $n = 4654$ cells; untreated_CTC, $n = 127$ cells. One-way analysis of variance (ANOVA) was performed using the Kruskal–Wallis method, and the Mann–Whitney test was used to compare differences between groups.*$P < 0.05$, **$P < 0.01$, ***$P < 0.001$, ****$P < 0.0001$.

	Histology				Histology			
	Overall	P-SCLC	NSCLC	*P* value	Overall	P-SCLC	C-SCLC	*P* value
		n = 80	n = 73			n = 80	n = 27	
–	73 (47.71)	28 (35.00)	45 (61.64)	<0.001***	48 (44.86)	28 (35.00)	20 (74.07)	<0.01**
1+	47 (30.72)	26 (32.50)	21 (28.77)		29 (27.10)	26 (32.50)	3 (11.11)	
2+	29 (18.95)	22 (27.50)	7 (9.59)		26 (24.30)	22 (27.50)	4 (14.81)	
3+	4 (2.61)	4 (5.00)	0 (00.00)		4 (3.74)	4 (5.00)	0 (00.00)	
Total	80 (52.29)	52 (65.00)	28 (38.36)	<0.01**	59 (55.14)	52 (65.00)	7 (25.93)	<0.001***

For p-SCLC group, c-SCLC group and NSCLC group, n = 80, 27 and 73 samples were evaluated. Data represent ATAD2 expression in the CHCAMS cohort determined by IHC (percentages). IHC showed that ATAD2 expression was statistically significantly higher in 80 p-SCLC patient specimens (65.0%), 27 c-SCLC patient specimens (25.93%) ($P = 0.0009$) and 73 NSCLC patient tissues (38.36%) ($P = 0.001727$). Statistical comparisons were performed using Chi-square test. *$P < 0.05$, **$P < 0.01$, ***$P < 0.001$.

Table 1: **Quantification of ATAD2 expression in the CHCAMS cohort determined by IHC.**

sites were inconsistent (Supplementary Table S3). The YSDDDVPSV is consistent with the peptide sequence of ATAD2 from the UniProt database (Supplementary Fig. S5B) and was detected in three SCLC models, including SCLC-A (H69), SCLC-N (H82), and SCLC-Y (DMS114), two of which harbor HLA-I sites HLA-A*02:01. Moreover, YSDDDVPSV was predicted to have strong binding affinity for TCR (EL_rank = 0.115). To test whether YSDDDVPSV could activate T cells, we isolated PBMCs from two normal healthy volunteers with two different HLA genotypes: HLA-A*02:01 present and HLA-A*02:01 absent (non-HLA-A*02:01) (Fig. 4B). Enrichment and expansion of IFN-γ-secreting $CD8^+$ T cells was performed by stimulating HLA-A*02:01 and non-HLA-A*02:01 PBMCs with two rounds of T2 cells pulsed with the YSDDDVPSV peptide for 9 days. The percentage of activated $CD8^+$ T cells that could secrete IFN-γ was quantified by ICS. A much higher percentage of IFN-γ-secreting $CD8^+$ T cells was observed in HLA-A*02:01 cultures (16.3%) compared to non- HLA-A*02:01 cultures (1.66%) ($P < 0.01$**) (Fig. 4C). To further validate this finding, we used CBA to detect IFN-γ in culture supernatants, and we found higher levels of IFN-γ in the culture supernatant from HLA-A*02:01 T cells than that from non-HLA-A*02:01 T cells (834 pg/ml versus 497 pg/ml) (Table 3), although both were statistically different from that of the control group ($P = 0.0047$ and $P = 0.0001$, respectively) (Fig. 4D). However, this result in combination with the results of the ICS assay suggest that IFN-γ-secreting T cells from non-HLA-A*02:01 PBMCs were not CTLs (Fig. 4C). Taken together, our results suggest that the HLA-A*02:01-YSDDDVPSV immunopeptide could stimulate T cell activation in an HLA-dependent manner and provides rationale for further study of this as an immune drug target in SCLC.

	ATAD2			
	Overall	positive	negative	*P* value
SCLC-ASCL1 (%)	**n = 80**	**52 (65.00)**	**28 (35.00)**	
–	27 (33.75)	9 (17.30)	18 (64.28)	<0.0001****
1+	22 (27.50)	20 (38.46)	2 (7.14)	
2+	26 (32.50)	19 (17.30)	7 (25.00)	
3+	5 (6.25)	4 (7.69)	1 (3.57)	
Total	53 (66.25)	43 (82.69)	10 (35.71)	<0.0001****
SCLC-NEUROD1 (%)	**n = 80**	**52 (65.00)**	**28 (35.00)**	
–	32 (40.00)	18 (34.61)	14 (50.00)	0.404
1+	18 (22.50)	14 (26.92)	4 (14.28)	
2+	23 (28.75)	16 (30.76)	8 (28.57)	
3+	6 (7.50)	4 (7.69)	2 (7.14)	
Total	48 (60.00)	34 (65.38)	14 (50.00)	0.301
SCLC-POU2F3 (%)	**n = 80**	**52 (65.00)**	**28 (35.00)**	
–	76 (95.00)	49 (94.23)	27 (96.42)	1.000
1+	3 (3.75)	2 (3.84)	1 (3.57)	
2+	1 (1.25)	1 (1.92)	0 (00.00)	
3+	0 (00.00)	0 (00.00)	0 (00.00)	
Total	4 (5.00)	3 (5.76)	1 (00.00)	1.000
SCLC-YAP1 (%)	**n = 80**	**52 (65.00)**	**28 (35.00)**	
–	73 (91.25)	47 (90.38)	26 (92.85)	1.000
1+	4 (5.00)	3 (5.76)	1 (3.57)	
2+	3 (3.75)	2 (3.84)	1 (3.75)	
3+	0 (00.00)	0 (00.00)	0 (00.00)	
Total	7 (8.75)	5 (9.61)	2 (7.14)	1.000
SCLC-MIX (%)	**n = 80**	**52 (65.00)**	**28 (35.00)**	
MIX	12 (15.00)	4 (7.69)	8 (28.57)	<0.05*
Non-MIX	68 (5.00)	48 (92.30)	20 (71.42)	

For each group, n = 80 samples were evaluated. Data represent correlation between ATAD2 expression and expression of ANPY subtype markers (percentage is positivity). Statistical comparisons were performed using the chi-square test. *$P < 0.05$, **$P < 0.01$, ***$P < 0.001$, ****$P < 0.0001$. Bold indicates ATAD2 expression in patients with 80 p-SCLC.

Table 2: **Correlation between ATAD2 expression and expression of ANPY subtype markers.**

Discussion

At present, targetable antigens expressed by SCLC have not been identified, preventing the use of immunotherapy drugs for this indication. Over the past two decades, many TAAs have been discovered by studies employing next-generation sequencing, bioinformatics, and other approaches; among these, CTAs have attracted considerable interest[36,37] because they are highly expressed in tumour cells, testis, and placental tissues but hardly expressed in other normal tissues, making

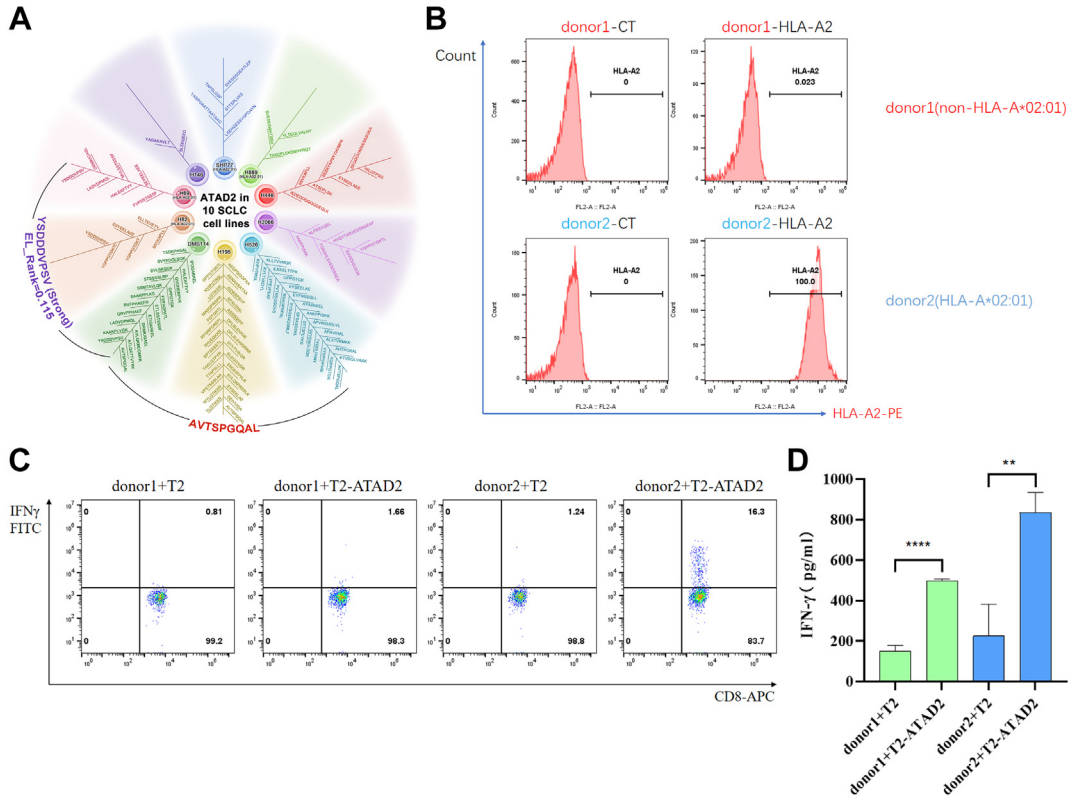

***Fig. 4*: Identification and characterization of YSDDDVPSV as a viable ATAD2 immunopeptide in HLA-I-expressing SCLC cell lines**. (A) Detection of 106 ATAD2 immunopeptides, represented by different colored dendrites, by LC–MS/MS analysis of ten HLA-I-expressing SCLC cell lines. YSDDDVPSV was expressed in H69, H82, and DMS114 cells, and AVTSPGQAL was expressed in H196, H526, and DMS114 cells. (B) Enrichment and expansion of IFN-γ-secreting $CD8^+$ T cells was performed by stimulating PBMCs from non-HLA-A*02:01 and HLA-A*02:01 with two rounds of T2 cells pulsed with the YSDDDVPSV peptide. (C) Bar plot showing amount of IFN-γ detected in the culture supernatant of cells in (B). $^{**}P = 0.0047$ and $^{****}P = 0.0001$. (D) The percentage of activated $CD8^+$ T cells derived as described in (B) that could secrete IFN-γ (FITC-IFN-γ -stained) was quantified by ICS using APC-CD8 antibody staining.

them promising disease-specific antigenic targets with low risk of off-target toxicity. Recent studies have reported high HLA gene expression in SCLC-Y tumours, but this study did not perform a peptidomics analysis to determine how the expression pattern of CTA genes in this subtype may contribute to immunotherapy response.[11] In agreement with this, we found by LC–MS/MS analyses that expression patterns of CTAs differed significantly in SCLC subtypes. Ninety-nine of the 281 CTAs were detected in 11 SCLC cell lines—representing the spectrum of five subtypes (SCLC-A/N/Y/P and -mixed)—and there were six common CTAs shared among the 11 SCLC cell lines. Four out of these six CTAs were also present in clinical SCLC specimens. These results confirm the documented heterogeneity of SCLC and underscore the need to identify common tumour antigens across SCLC subtypes to enable immunotherapy approaches.

ATAD2, one of the four common CTAs identified in both SCLC cell lines and patient tissues, was expressed at significantly higher levels in than in matched normal-adjacent tissue or in NSCLC tissues. Interestingly, we also found that *ATAD2* expression pattern was significantly different among SCLC subtypes: *ATAD2* expression was significantly higher in SCLC-A/N models compared to SCLC-P/Y/MIX models. Moreover, *ATAD2* expression was positively correlated with *ASCL1* expression and negatively correlated SCLC-MIX expression, but no relationship was found between *ATAD2* expression and *NEUROD1*, *POU2F3*, and *YAP1*. These data suggest that *ATAD2* may serve as a potential tumour antigen target for SCLC-A and SCLC-N SCLC subtypes; however, there are no reports of ATAD2 as an immunotherapy target in SCLC.

It has been shown that, in SCLC, the expression of MHC-I is negatively correlated with LSD1, and LSD1 is positively correlated with ASCL1.[38] It was further shown that, in SCLC-A/N, the expression of both MHC-I and APM is lower than in SCLC-P/Y. In clinical studies of

Summary report

Name	Dilution	IL-5	IFN-α	IL-2	IL-6	IL-18	IL-10	IFN-γ	IL-8	IL-17	IL-4	IL-12P70	TNF-α
donor1+T2_1.fcs	1	<2.06	<1.18	7.76	9.24	<1.81	<0.97	136.8	5.76	<1.00	10.57	<2.00	9.76
donor1+T2_2.fcs	1	<2.06	<1.18	9.94	12.1	<1.81	<0.97	183.28	5.05	<1.00	14.77	<2.00	10.67
donor1+T2_3.fcs	1	<2.06	<1.18	7.1	8	<1.81	<0.97	127.82	5	<1.00	10.11	<2.00	8.54
donor1+T2-ATAD2_1.fcs	1	2.25	<1.18	23.03	1.04	<1.81	1.29	484.37	4.54	1.01	2.31	<2.00	6.84
donor1+T2-ATAD2_2.fcs	1	2.77	<1.18	25.2	1.45	<1.81	1.46	504.87	6.01	<1.00	<1.54	<2.00	7.45
donor1+T2-ATAD2_3.fcs	1	2.66	<1.18	27.2	1.35	<1.81	1.27	501.01	7.45	1.06	<1.54	<2.00	9.97
donor2+T2_1.fcs	1	23.09	<1.18	3.67	61.89	3.18	1.15	295.71	11.4	1.04	17.09	<2.00	14.18
donor2+T2_2.fcs	1	4.46	<1.18	1.53	14.65	<1.81	<0.97	46.58	6.12	<1.00	18.85	<2.00	4.2
donor2+T2_3.fcs	1	104.5	1.21	9.84	176.1	8.88	1.11	334.38	7.98	<1.00	154.96	<2.00	27.2
donor2+T2-ATAD2_1.fcs	1	23.7	<1.18	8.75	1.37	<1.81	1.4	934.32	8.84	<1.00	<1.54	<2.00	8.72
donor2+T2-ATAD2_2.fcs	1	22.67	<1.18	7.33	1.34	<1.81	1.3	833.54	6.39	<1.00	<1.54	<2.00	7.71
donor2+T2-ATAD2_3.fcs	1	20.66	<1.18	7.22	1.4	<1.81	1.27	735.1	7.95	<1.00	1.86	<2.00	8.47

Note: Final Sample Concentration (=diluted sample concentration multiplied dilution factor). Unit: pg/ml.

***Table 3*: Concentration of cytokines in supernatant of CD8$^+$ T cell cultures derived from HLA-A*02:01 and non-HLA-A*02:01 PBMCs.**

SCLC, the expression of APM was significantly elevated in SCLC-Y compared to other subtypes.[39] In the present study, we found that MHC-I expression of SCLC-A/N cell lines was significantly lower than that of SCLC-P/Y cell lines, and the number of CTAs and immunopeptides were significantly lower in SCLC-A/N cell lines than in SCLC-P/Y cell lines. While the MHC-I-enriched bands of SCLC-A (H69) cells were similar to those of SCLC-P/Y (Supplementary Fig. S2), there were significantly fewer CTAs and immunopeptides in H69 compared to H196, DMS114, and H526 (Supplementary Table S2), demonstrating that the number of CTAs and immunopeptides did not correlate with the expression of MHC-I. We also found fewer CTAs in scRNA-seq data of SCLC relapse tumours compared with primary tumours, although, interestingly, there were no novel CTAs in detected in any of the relapse tumours. We demonstrated that the number of CTAs and immunopeptides in the SCLC-A/N subtypes were significantly lower than those in SCLC-P/Y subtypes, which, in addition to being affected by the expression of MHC-I and APM, also may correlate with the occurrence of more severe immune escape in SCLC-A/N, leading to a decreased number of CTAs and their immunopeptides. As a result, decreased MHC-I and CTA expression in SCLC-A/N may leads to its poor response to immune-targeting drugs.

Among 100 ATAD2 immunopeptides detected in our models, YSDDDVPSV had the most favorable characteristics for immune targeting: it is nine amino acids long and has a non-polar hydrophobic valine at the C-terminal (carboxy-terminal) end, which is favorable for binding to the antigenic groove of the HLA-I molecule. Although YSDDDVPSV was reported to be present in THP-1 (acute monocyte leukemia), acute myeloid leukemia cell lines, and osteosarcoma,[40–44] no validation of T cell reactivity was performed in patient cohorts. In our study, we demonstrate that non-HLA-A*02:01 T cells were very weakly reactive to YSDDDVPSV-pulsed T2 cells, whereas HLA-A*02:01 T cells were strongly reactive. These results indicated that HLA-A*02:01-YSDDDVPSV antigenic peptide may be a potential target for future development of immunotherapies, especially for HLA-A*02:01-restricted patients with SCLC.

SCLC-A represents the largest percentage of SCLC, and the majority of SCLC expressed ASCL1. *ATAD2* expression is positively correlated with the expression of *ASCL1*, and YSDDDVPSV immunopeptides are present in SCLC-A and SCLC-N with HLA-A*02:01 restriction. TCR-T is an a type of ACT therapy that is generating great excitement in the field of tumour immunotherapy, and selection of an appropriate tumour antigen target is key to developing safe and effective TCR-T cell therapies. Due to the diversity of SCLC typing protocols as well as the potential for converting between subtypes, it is indeed important to consider the treatment efficacy profile of patients with SCLC subtype switching.[45,46] The amount of YSDDDVPSV ATAD2 immunopeptide, as well as the expression of ATAD2, varies widely among SCLC subtypes. Some studies have shown that patients with SCLC-Y or SCLC-I have increased response to PD-1/PD-L1 inhibitors. SCLC-P is weakly positive for ATAD2 expression, suggesting that YSDDDVPSV ATAD2 immunopeptide-based TCR-T cell therapy could also be used, although the low ATAD2 expression levels could affect the efficacy and require adjustments to the design of the relevant TCR-T will be considered to optimize its efficacy. In our ongoing research, we are modifying TCRs with ATAD2-derived YSDDDVPSV immune peptides to construct TCR-T cells and test their ability to kill SCLC tumour cells. If successful, this approach could benefit most patients with SCLC-A harboring HLA-A*02:01 as well as patients with complex SCLC subtypes that express ASCL1.

Contributors

Jie Wang, Zhijie Wang, Jianchun Duan and Li Yuan: Funding acquisition, Supervision.

Jie Wang: conceptualization, revision of the manuscript.

Li Yuan: conceptualization, literature searches, methodology, Formal analysis, Investigation, writing original draft preparation.

Sini Li, Yixiang Zhu, Xue Zhang, Yan Qu, Lin Yang, Zheng Liu and Yanhua Tian: methodology, formal analysis, investigation.

Sini Li, Jia Zhong, Jian Zhang, Yan He, Yufeng Guo, Dan Ming He, Wei Zhuang, Jinsong Zhang, Zixiao Ma and Hua Bai: literature searches, writing—review and editing.

Yixiang Zhu, Lihui Liu, Boyang Sun and Kailun Fei: extraction data, evaluation study quality and bias risk of eligible trials.

Sini Li, Yixiang Zhu verified the underlying data. All authors read and approved the final manuscript.

Data sharing statement

The mass spectrometry proteomics data have been deposited to the ProteomeXchange Consortium (https://proteomecentral.proteomexchange.org) via the iProX partner repository with the dataset identifier PXD058303. The project is currently in plan to public (public start date: February 01, 2025) status. The single-cell RNA sequencing (scRNA-seq) data from human SCLC lung tissues were retrieved from the Genome Sequence Archive database of the National Genomics Data Center (https://bigd.big.ac.cn/) under the BioProject accession code: PRJCA006026. GSM4104155 (untreated CTC), GSM4104156 (cisplatin CTC), GSM4104157 (cisplatin relapsed CTC), and GSM4104163 (untreated CDX) single-cell data were downloaded from the Gene Expression Omnibus (GEO) database under accession number GSE138267. The National Cancer Institute (NCI) SCLC cell line expression data were downloaded from the GEO (GSE73160). Gene expression data with accession numbers GSE43346 and GSE40275 were downloaded from the GEO. mRNA-seq data of SCLC patients were downloaded from cBioPortal database (U Cologne, Nature 2015).

Declaration of interests

The authors declare that they have no competing interests.

Acknowledgements

The authors thank all the patients for tissue donation and all health volunteers for PBMC in this study.We thank all the Jie Wang lab members for technical support and sharing data. This study was supported by the National key R&D program of China (2022YFC2505000); National Natural Science Foundation of China (NSFC) general program (82272796); NSFC special program (82241229); CAMS Innovation Fund for Medical Sciences(CIFMS 2022-I2M-1-009); CAMS Key Laboratory of Translational Research on Lung Cancer (2018PT31035); Aiyou foundation (KY201701); National key R&D program of China (2022YFC2505004); NSFC general program (81972905); Medical Oncology Key Foundation of Cancer Hospital Chinese Academy of Medical Sciences (CICAMS-MOCP2022012).

Appendix A. Supplementary data

Supplementary data related to this article can be found at https://doi.org/10.1016/j.ebiom.2024.105515.

References

1 Rudin CM, Brambilla E, Faivre-Finn C, Sage J. Small-cell lung cancer. *Nat Rev Dis Primers*. 2021;7(1):3.
2 Farago AF, Keane FK. Current standards for clinical management of small cell lung cancer. *Transl Lung Cancer Res*. 2018;7:69–79.
3 Horn L, Mansfield AS, Szczęsna A, et al. First-line atezolizumab plus chemotherapy in extensive-stage small-cell lung cancer. *N Engl J Med*. 2018;379(23):2220–2229.
4 Reck M, Luft A, Szczesna A, et al. Phase III randomized trial of ipilimumab plus etoposide and platinum versus placebo plus etoposide and platinum in extensive-stage small-cell lung cancer. *J Clin Oncol*. 2016;34:3740–3748.
5 Liu SV, Reck M, Mansfield AS, et al. Updated overall survival and PD-L1 subgroup analysis of patients with extensive-stage small-cell lung cancer treated with Atezolizumab, carboplatin, and etoposide (IMpower133). *J Clin Oncol*. 2021;39(6):619–630.
6 Goldman JW, Dvorkin M, Chen Y, et al. Durvalumab, with or without tremelimumab, plus platinum-etoposide versus platinum-etoposide alone in first-line treatment of extensive-stage small-cell lung cancer (CASPIAN): updated results from a randomized, controlled, open-label, phase 3 trial. *Lancet Oncol*. 2021;22(1):51–65.
7 Wang J, Zhou C, Yao W, et al. Adebrelimab or placebo plus carboplatin and etoposide as first-line treatment for extensive-stage small-cell lung cancer (CAPSTONE-1): a multicentre, randomized, double-blind, placebo-controlled, phase 3 trial. *Lancet Oncol*. 2022;23(6):739–747.
8 Tian Y, Wang J, Tang F. Single-cell transcriptomic profiling reveals the tumour heterogeneity of small-cell lung cancer. *Signal Transduct Target Ther*. 2022;7(1):346.
9 Rudin CM, Poirier JT, Byers LA, et al. Molecular subtypes of small cell lung cancer: a synthesis of human and mouse model data. *Nat Rev Cancer*. 2019;19(5):289–297.
10 Qu S, Fetsch P, Thomas A, et al. Molecular subtypes of primary SCLC tumors and their associations with neuroendocrine and therapeutic markers. *J Thorac Oncol*. 2022;17(1):141–153.
11 Gay CM, Stewart CA, Park EM, et al. Patterns of transcription factor programs and immune pathway activation define four major subtypes of SCLC with distinct therapeutic vulnerabilities. *Cancer Cell*. 2021;39(3):346–360.e7.
12 Owonikoko TK, Dwivedi B, Chen Z, et al. YAP1 expression in SCLC defines a distinct subtype with T-cell-inflamed phenotype. *J Thorac Oncol*. 2021;16(3):464–476.
13 Zhang P, Zhang G, Wan X. Challenges and new technologies in adoptive cell therapy. *J Hematol Oncol*. 2023;16:97.
14 Shao W, Yao Y, Yang L, et al. Novel insights into TCR-T cell therapy in solid neoplasms: optimizing adoptive immunotherapy. *Exp Hematol Oncol*. 2024;13:37.
15 Harris DT, Hager MV, Smith SN, et al. Comparison of T Cell activities mediated by human TCRs and CARs that use the same recognition domains. *J Immunol*. 2018;200:1088–1100.
16 Xu Y, Yang Z, Horan LH, et al. A novel antibodyTCR (AbTCR) platform combines Fab-based antigen recognition with gamma/delta-TCR signaling to facilitate T-cell cytotoxicity with low cytokine release. *Cell Discov*. 2018;4:62.
17 Xu R, Du S, Zhu J, Meng F, Liu B. Neoantigen-targeted TCR-T cell therapy for solid tumours: how far from clinical application. *Cancer Lett*. 2022;546:215840.
18 Sivakumar S, Moore JA, Montesion M, et al. Integrative analysis of a large real-world cohort of small cell lung cancer identifies distinct genetic subtypes and insights into histologic transformation. *Cancer Discov*. 2023;13(7):1572–1591.
19 Sammut SJ, Feichtinger J, Stuart N, Wakeman JA, Larcombe L, McFarlane RJ. A novel cohort of cancer-testis biomarker genes revealed through meta-analysis of clinical data sets. *Oncoscience*. 2014;1(5):349–359.
20 Carey TE, Takahashi T, Resnick LA, Oettgen HF, Old LJ. Cell surface antigens of human malignant melanoma: mixed hemadsorption assays for humoral immunity to cultured autologous melanoma cells. *Proc Natl Acad Sci U S A*. 1976;73:3278–3282.
21 Scanlan MJ, Simpson AJ, Old LJ. The cancer/testis genes: review, standardization, and commentary. *Cancer Immun*. 2004;4:1.
22 Hong DS, Van Tine BA, Biswas S, et al. Autologous T cell therapy for MAGE-A4+ solid cancers in HLA-A*02+ patients: a phase 1 trial. *Nat Med*. 2023;29(1):104–114. https://doi.org/10.1038/s41591-022-02128-z.
23 Pan Q, Weng D, Liu J, et al. Phase 1 clinical trial to assess safety and efficacy of NY-ESO-1-specific TCR T cells in HLA-A*02:01 patients with advanced soft tissue sarcoma. *Cell Rep Med*. 2023;4(8):101133.
24 Fouret R, Laffaire J, Hofman P, et al. A comparative and integrative approach identifies ATPase family, AAA domain containing 2 as a likely driver of cell proliferation in lung adenocarcinoma. *Clin Cancer Res*. 2012;18(20):5606–5616.
25 Lu WJ, Chua MS, So SK. Suppression of ATAD2 inhibits hepatocellular carcinoma progression through activation of p53-and p38-mediated apoptotic signaling. *Oncotarget*. 2015;6(39):41722.
26 Fruman DA, Rommel C. PI3K and cancer: lessons, challenges and opportunities. *Nat Rev Drug Discov*. 2014;13(2):140–156.

27 Dong P, Maddali MV, Srimani JK, et al. Division of labour between Myc and G1 cyclins in cell cycle commitment and pace control. *Nat Commun*. 2014;5(1):1–11.
28 Clark AG, Vignjevic DM. Modes of cancer cell invasion and the role of the microenvironment. *Curr Opin Cell Biol*. 2015;36:13–22.
29 De Amicis F, Chimento A, Montalto FI, Casaburi I, Sirianni R, Pezzi V. Steroid receptor signallings as targets for resveratrol actions in breast and prostate cancer. *Int J Mol Sci*. 2019;20(5):1087.
30 Koo SJ, Fernández-Montalván AE, Badock V, et al. ATAD2 is an epigenetic reader of newly synthesized histone marks during DNA replication. *Oncotarget*. 2016;7(43):70323.
31 van't Veer LJ, Dai H, Van de Vijver MJ, et al. Gene expression profiling predicts clinical outcome of breast cancer. *Nature*. 2002;415(6871):530–536.
32 Zhang MJ, Zhang CZ, Du WJ, Yang XZ, Chen ZP. ATAD2 is overexpressed in gastric cancer and serves as an independent poor prognostic biomarker. *Clin Transl Oncol*. 2016;18(8):776–781.
33 Liu N, Funasaka K, Obayashi T, et al. ATAD2 is associated with malignant characteristics of pancreatic cancer cells. *Oncol Lett*. 2019;17(3):3489–3494.
34 Hussain M, Zhou Y, Song Y, et al. ATAD2 in cancer: a pharmacologically challenging but tractable target. *Expert Opin Ther Targets*. 2018;22(1):85–96.
35 Hikmet F, Rassy M, Backman M, et al. Expression of cancer-testis antigens in the immune microenvironment of non-small cell lung cancer. *Mol Oncol*. 2023;17(12):2603–2617. https://doi.org/10.1002/1878-0261.13474.
36 Simpson AJ, Caballero OL, Jungbluth A, Chen YT, Old LJ. Cancer/testis antigens, gametogenesis and cancer. *Nat Rev Cancer*. 2005;5:615e25.
37 Almeida LG, Sakabe NJ, deOliveira AR, et al. CTdatabase: a knowledge-base of high-throughput and curated data on cancer-testis antigens. *Nucleic Acids Res*. 2009;37:D816e9.
38 Nguyen EM, Taniguchi H, Rudin CM, et al. Targeting lysine-specific demethylase 1 rescues major histocompatibility complex class I antigen presentation and overcomes programmed death-ligand 1 blockade resistance in SCLC. *J Thorac Oncol*. 2022;17(8):1014–1031.
39 Rudin CM, Balli D, Lai WV, et al. Clinical benefit from immunotherapy in patients with SCLC is associated with tumour capacity for antigen presentation. *J Thorac Oncol*. 2023;18(9):1222–1232.
40 Jensen SM, Potts GK, Patterson MJ, Patterson MJ. Specific MHC-I peptides are induced using PROTACs. *Front Immunol*. 2018;9:2697.
41 Scull KE, Pandey K, Purcell AW, Purcell AW. Immunopeptidogenomics: harnessing RNA-seq to illuminate the dark immunopeptidome. *Mol Cell Proteomics*. 2021;20:100143. https://doi.org/10.1016/j.mcpro.2021.100143.
42 Pandey K, Mifsud NA, Lim Kam Sian TCC, et al. In-depth mining of the immunopeptidome of an acute myeloid leukemia cell line using complementary ligand enrichment and data acquisition strategies. *Mol Immunol*. 2020;123:7–17.
43 Vadakekolathu J, Boocock DJ, Pandey K, et al. Multi-Omic analysis of two common P53 mutations: proteins regulated by mutated P53 as potential targets for immunotherapy. *Cancers (Basel)*. 2022;14(16):3975.
44 Klatt MG, Mack KN, Bai Y, et al. Solving an MHC allele-specific bias in the reported immunopeptidome. *JCI Insight*. 2020;5(19):e141264.
45 Lo YC, Rivera-Concepcion J, Vasmatzis G, Aubry MC, Leventakos K. Subtype of SCLC is an intrinsic and persistent feature through systemic treatment. *JTO Clin Res Rep*. 2023;4(9):100561.
46 Voigt E, Wallenburg M, Wollenzien H, et al. Sox 2 is an oncogenic driver of small-cell lung cancer and promotes the classic neuroendocrine subtype. *Mol Cancer Res*. 2021;19(12):2015–2025.